Model-Based Deduction of CMYK Surface Coverages from Visible and Infrared Spectral Measurements of Halftone Prints

Thomas Bugnon, Mathieu Brichon and Roger David Hersch
Ecole Polytechnique Fédérale de Lausanne (EPFL),
School of Computer and Communication Sciences, Lausanne 1015, Switzerland

ABSTRACT

The Yule-Nielsen modified Spectral Neugebauer reflection prediction model enhanced with an ink spreading model provides high accuracy when predicting reflectance spectra from ink surface coverages. In the present contribution, we try to inverse the model, i.e. to deduce the surface coverages of a printed color halftone patch from its measured reflectance spectrum. This process yields good results for cyan, magenta, and yellow inks, but unstable results when simultaneously fitting cyan, magenta, yellow, and black inks due to redundancy between these four inks: black can be obtained by printing either the black ink or similar amounts of the cyan, magenta, and yellow inks. To overcome this problem, we use the fact that the black pigmented ink absorbs light in the infrared domain, whereas cyan, magenta, and yellow inks do not. Therefore, with reflection spectra measurements spanning both the visible and infrared domain, it is possible to accurately deduce the black ink coverage. Since there is no redundancy anymore, the cyan, magenta, yellow, and pigmented black ink coverages can be recovered with high accuracy.

Keywords: color reproduction, spectral prediction model, infrared reflection spectra, ink surface coverages, color halftones

1. INTRODUCTION

The goal of a color reproduction system is to be able to reproduce input colors as accurately as possible. This is not a trivial task since the human visual system is very sensitive to small color differences. In printing systems, there are many factors influencing the range of printable colors such as the inks, the substrate (paper, plastic, glass, etc.), the illumination conditions, and the halftones. Spectral reflection prediction models are helpful in studying these different influences.

Spectral reflection prediction models allow predicting reflectance spectra in function of the ink surface coverages. Such predictions, further referred to as *forward predictions*, can be accurately performed for four or more inks[1]. Inversing the models, i.e. deducing the ink surface coverages from a given printed color patch, is an important building stone for applications such as optimizing GCR parameters. Working with four inks, i.e. cyan, magenta, yellow, and black, current models cannot easily perform *inverse* or *backward predictions*, i.e. deduce the ink surface coverages from a given printed color patch.

The aim of this paper is to show why it is hard to perform inverse predictions with four inks and how we can improve such predictions using spectra spanning both the visible and infrared domain. We focus on classical cyan, magenta, yellow, and black color halftone patches printed on paper. The measurements used for the experiments were made on color patches printed on a web offset press. Classical rotated halftone screens were printed at 100 lpi. The colors printed were all the combinations of cyan, magenta, and yellow inks at surface coverages of 0%, 25%, 50%, 75%, or 100% and black ink at surface coverages of 0%, 10%, 30%, 50%, 80%, or 100%, creating a set of 750 different colors.

Section 2 introduces the Yule-Nielsen modified Spectral Neugebauer model enhanced with an ink spreading model[1] that we use for deducing surface coverages from reflection spectra. The limitations of this model for recovering the cyan, magenta, yellow and black surface coverages are presented in Section 3. In Section 4, we provide a solution to the problem by extending the considered wavelength range to the infrared domain and show in Section 5 how the consistency of this new model is improved. We finally draw the conclusions in Section 6.

Proc. SPIE Vol. 6493, 649310, Color Imaging XII: Processing, Hardcopy, and Applications; Reiner Eschbach, Gabriel G. Marcu; Eds., January 2007

2. SPECTRAL PREDICTION MODELS AND RELATED APPROACHES

Many different phenomena influence the reflection spectrum of a color halftone patch printed on a diffusely reflecting substrate (e.g. paper). These phenomena comprise the surface (Fresnel) reflection at the interface between the air and the paper, light scattering and reflection within the substrate (i.e. the paper bulk), and the internal (Fresnel) reflections at the interface between the paper and the air.

The lateral scattering of light within the paper substrate and the internal reflections at the interface between the paper and the air are responsible for what is generally called the optical dot gain, also known as the Yule-Nielsen effect. In addition, due to the printing process, deposited ink surface coverages are generally larger than nominal coverages, yielding a physical dot gain also referred to as mechanical dot gain. Such effective ink surface coverages depend on the inks, the paper, and also the specific ink superposition conditions, i.e. the superposition of ink halftones and solid inks.

At the present time and according to the literature[3, 4, 5], mainly the well-known Yule-Nielsen modified Spectral Neugebauer model[6, 7] seems to be used in practice. Many other spectral prediction models allow the exploration of various effects, but are too complex, not accurate enough, or not comprehensive enough to be usable in practice.

2.1. The Yule-Nielsen modified Spectral Neugebauer model

One of the first spectral models is the Neugebauer model[8]. In its original form, it predicts the CIE-XYZ tri-stimulus values of a color halftone patch as the sum of the tri-stimulus values of their individual colorants weighted by their fractional area coverages a_i. By considering the reflection spectra R_i of colorants instead of their respective tri-stimulus values, one obtains the spectral Neugebauer equations. They predict the reflection spectrum of a printed color halftone patch as a function of the reflection spectra of its individual colorants (also called Neugebauer primaries):

$$R(\lambda) = \sum_i a_i * R_i(\lambda) \tag{1}$$

With k inks, there are 2^k colorants: white, the k single ink colorants and all the different superpositions of solid inks. For example, the red colorant is the superposition of the magenta and yellow inks. When the ink layers are printed independently one from another, the fractional area coverages of the individual colorants are closely approximated from the ink surface coverages by the Demichel equations[9]. These equations are shown in Figure 1 for the case of 2 inks, but can be extended to accommodate any number of inks[1].

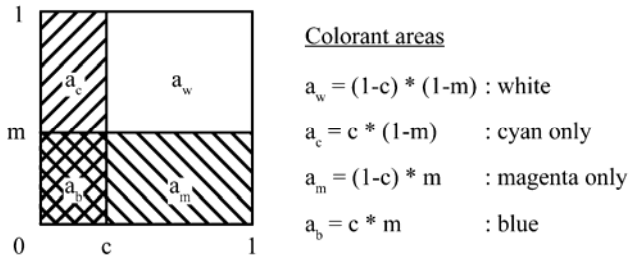

Figure 1. Demichel equations for 2 inks: cyan (c) and magenta (m).

The Neugebauer model is a generalization of the Murray-Davis model[10] whose colorants are formed by only one ink and the paper white. Since the Neugebauer model neither takes explicitly into account the lateral propagation of light within the paper bulk nor the internal reflections (Fresnel reflections) at the paper-air interface, its predictions are not accurate[11]. Yule and Nielsen[6] modeled the non-linear relationship between the reflectance of paper, single ink halftones, and solid inks by a power function whose exponent n can be optimized according to the reflectance of a limited set of color patches. Viggiano[7] applied the Yule-Nielsen relationship to the spectral Neugebauer equations, yielding the Yule-Nielsen modified Spectral Neugebauer model (YNSN):

$$R(\lambda) = \left(\sum_i a_i * R_i(\lambda)^{\frac{1}{n}} \right)^n \tag{2}$$

This YNSN model has been used by many researchers for the characterization of printing systems[4, 7, 11, 13, 14, 15, 16]. This model therefore plays a significant role in building color management systems.

2.2. The Ink Spreading Enhanced Yule-Nielsen modified Spectral Neugebauer (EYNSN)

One of the latest models is the Yule-Nielsen modified Spectral Neugebauer model enhanced with an ink spreading model (EYNSN)[1, 2]. Ink spreads out differently according to the ink superposition condition. The amount of dot gain depends on whether an ink halftone is printed alone on paper or in superposition with one or more other inks. The YNSN has therefore been enhanced to account for this phenomenon.

Forward predictions using the EYNSN are performed according to Figure 2. First, the effective single ink halftone surface coverages for the contributing superposition conditions are determined from nominal surface coverages by using the tone reproduction curves established during model calibration. There is one curve for each ink halftone in each superposition condition, i.e. an ink halftone superposed with one, two, or three given solid inks. In order to obtain the effective surface coverages of a color halftone patch, the previously computed effective single ink halftone surface coverages are weighted according to the surface coverages of the colorants contributing to that color halftone. With the Demichel equations, we can then compute the effective surface coverages of the colorants forming the ink halftone. Finally, the YNSN model computes the predicted reflection spectrum from these effective colorant coverages.

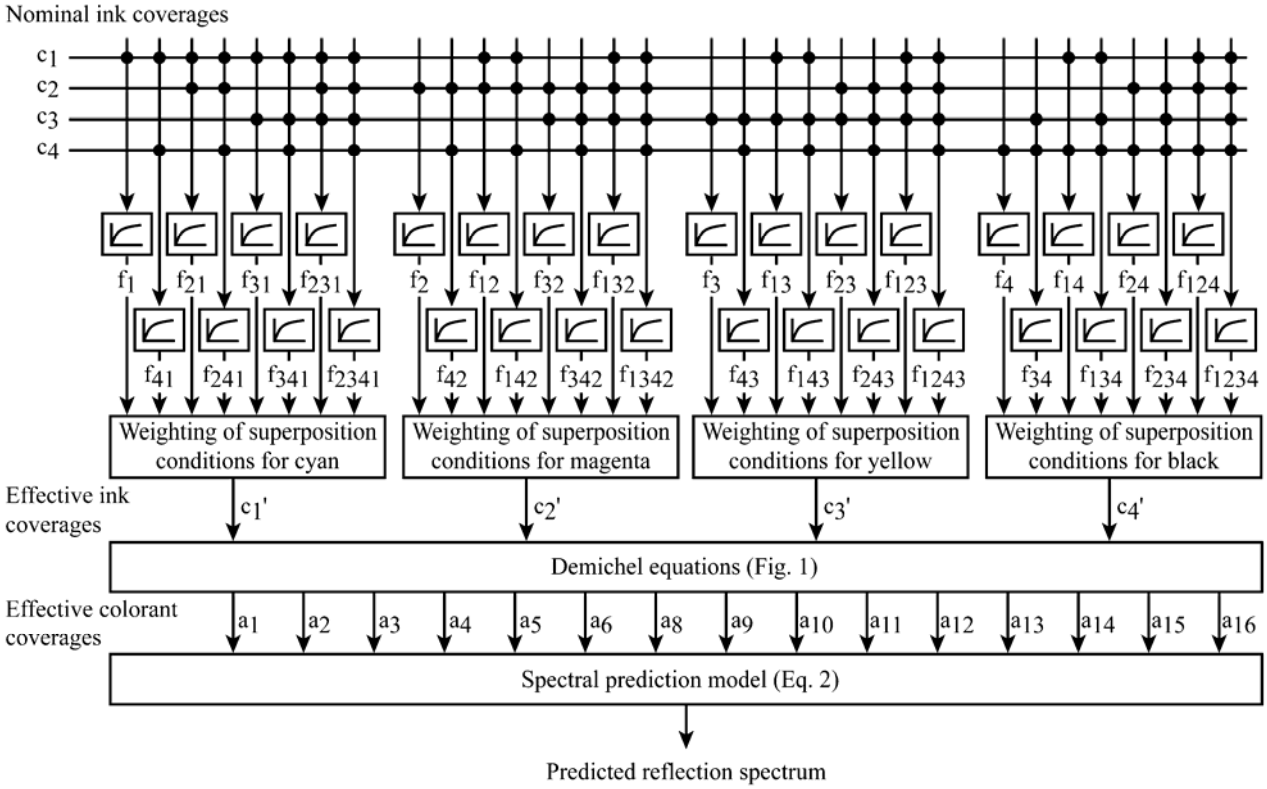

Figure 2. The Ink Spreading Enhanced Yule-Nielsen modified Spectral Neugebauer model with c_1, c_2, c_3, and c_4 the nominal ink surface coverages; $f_{j,k,i}$ the surface coverage of ink i superposed with solid inks j and k; c_1', c_2', c_3', and c_4' the effective ink surface coverages; and a_1 to a_{16} the effective colorant surface coverages.

Note that it is possible to replace the Yule-Nielsen modified Spectral Neugebauer model (Eq. 2) by a Clapper-Yule model[1] extended to account for middle and low screen frequencies.

Backward predictions are performed using optimization procedures[17, 18]: The optimization algorithm is asked to find the effective ink surface coverages that best fit the given spectrum. The resulting effective coverages yield the predicted spectrum that has the minimal distance to the given measured spectrum in terms of a given difference metric, e.g. the square Euclidian distance between reflection density spectra vectors.

3. LIMITATIONS OF THE VISIBLE DOMAIN

With the rods and cones, the human eye perceives light whose wavelength ranges from 400 nm to 700 nm. The cones are responsible for the perception of colors. There are three types of cones: the L, M and S cones which have a high sensibility in the red, green and blue wavelength ranges, respectively. Many printing systems therefore use cyan, magenta and yellow inks to reproduce colors because they absorb red, green and blue, respectively. This enables printing systems to reproduce a large part of the colors that the human visual system can see. Since each ink absorbs in a different spectral region, it is relatively easy with the EYNSN model to deduce the surface coverages of inks needed to reproduce a given color. One may for example add a stage converting reflection spectra to CIELAB coordinates and search for the surface coverages of the cyan, magenta and yellow inks minimizing the ΔE_{94} difference[19] between the desired and predicted colors.

In printed systems, in order to reduce the amounts of superposed cyan, magenta, and yellow inks, a fourth ink, black, is introduced. By performing gray component replacement (GCR), a given amount of black replaces the superposition of similar amounts of cyan, magenta, and yellow inks. One may create the black color either by superposing the cyan, magenta, and yellow inks, referred to as *chromatic black*, or by using the black ink, referred to as *pure black*. The spectra of the two black colors are shown in Figure 3. We can see that the two spectra do not yield the same color, i.e. the same black. For the considered web offset press technology, pure black is darker than chromatic black. Moreover, its spectrum is flatter, which ensures that it is really black and not slightly colored.

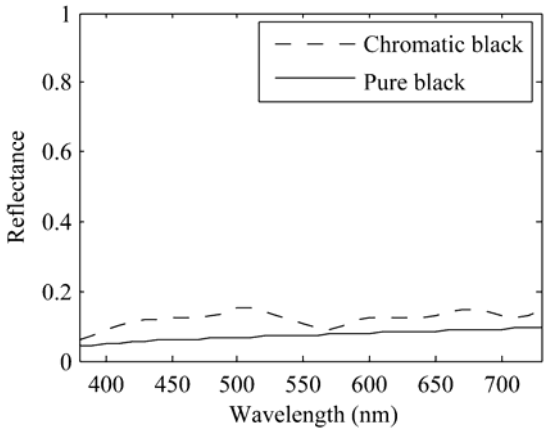

Figure 3. Reflection spectra of the chromatic and pure black printed colors.

Spectral prediction models can easily predict the reflection spectrum and therefore the resulting color given nominal ink surface coverages of the cyan, magenta, yellow and black inks[1, 2]. On the other hand, reversing the model when cyan, magenta, yellow and black inks are used, i.e. deducing the four effective ink surface coverages for a reflection spectrum, is much harder because of the redundancy between pure and chromatic black. It is indeed possible to achieve similar colors by replacing chromatic black with pure black and vice versa.

Let us show the redundancy between pure and chromatic black. In a first experiment, we try to reproduce 100% chromatic black, given by the superposition of solid cyan, solid magenta, and solid yellow, by using various relative

amounts of pure and chromatic black. We first choose the amount of pure black and then use the EYNSN spectral prediction model to deduce the amounts of cyan, magenta, and yellow inks reproducing the closest possible color to the desired chromatic black. We use the ΔE_{94} difference metric to evaluate the match[19]. With a ΔE_{94} difference below 1, since there is no noticeable difference for the human visual system, the match is perfect. With a ΔE_{94} difference below 3, the color match is reasonable and corresponds to current practices in web offset printing. Figure 4 shows that chromatic black can be reproduced with up to 75% of pure black, i.e. black ink, while keeping the ΔE_{94} difference below 1, i.e. without any noticeable difference for the human visual system. Moreover, we can use between 0% and 80% of pure black and keep the ΔE_{94} difference below 3. This interval is called the *$\Delta E_{94} \leq 3$ redundancy window*. In this experiment, the $\Delta E_{94} \leq 3$ redundancy window ranges from 0% to 80% and its width is 80%.

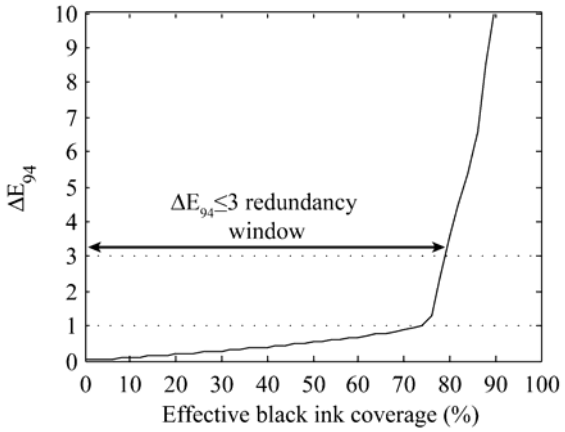

Figure 4. ΔE_{94} difference between 100% chromatic black and its closest color that can be reproduced using various relative amounts of pure and chromatic black. The ΔE_{94} difference is in function of the amount of pure black. The $\Delta E_{94} \leq 3$ redundancy window is also drawn.

The next experiment is performed on a color patch composed of 60% pure black. Again, we try to reproduce this color by using various relative amounts of pure and chromatic black. We first choose the amount of pure black and then use the EYNSN spectral prediction model to deduce the amounts of cyan, magenta, and yellow inks that reproduce the closest possible color to 60% pure black. Figure 5 shows that we have a $\Delta E_{94} \leq 3$ redundancy window ranging from 25% to 65% pure black. The color composed of 60% pure black can therefore be reproduced using only 25% pure black, which means that 35% pure black has been replaced by chromatic black.

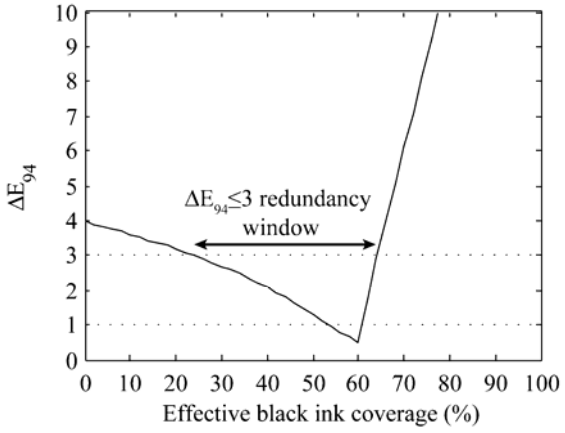

Figure 5. ΔE_{94} difference between 60% pure black and its closest color that can be reproduced using various relative amounts of pure and chromatic black. The ΔE_{94} difference is in function of the amount of pure black. The $\Delta E_{94} \leq 3$ redundancy window is also drawn.

Gray component replacement (GCR) is based on the redundancy between pure and chromatic black. Its goal is to replace to a certain extent chromatic black by pure black in order to limit the size of the areas covered by three superposed inks. GCR algorithms may replace all the chromatic black by pure black or only part of it. When GCR is applied, a given amount of pure black replaces a similar amount of chromatic black, i.e. similar amounts of cyan, magenta and yellow inks. Therefore, the sum of the pure black ink surface coverage and the maximum surface coverage of the cyan, magenta and yellow inks does not exceed 100%. Out of the 750 colors selected in Section 1, 245 colors match this criterion. Figure 6 shows the percentage of these 245 colors in function of the width of the $\Delta E_{94} \leq 3$ redundancy window. We can see that ¼ of the colors have a $\Delta E_{94} \leq 3$ redundancy window greater than 60% and ½ a $\Delta E_{94} \leq 3$ redundancy window greater than 40%.

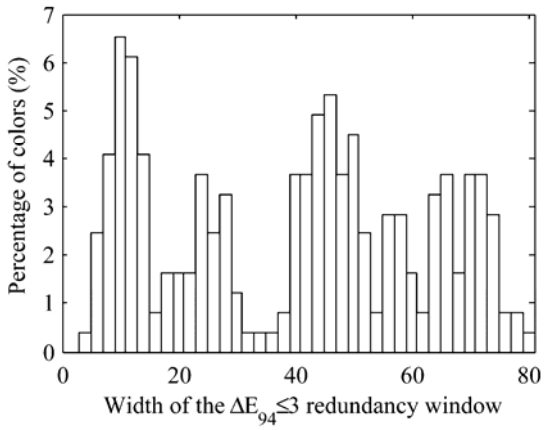

Figure 6. Percentage of colors in function of their $\Delta E_{94} \leq 3$ redundancy window.

When the $\Delta E_{94} \leq 3$ redundancy window of a color is wide, the effective ink surface coverages deduced by the EYNSN model for the given color are less accurate because the model is not able to distinguish between pure and chromatic black. Even if the deduced ink surface coverages reproduce the desired color for the human visual system, the low accuracy prevents recovering the exact ink surface coverages.

4. EXTENDING THE SPECTRAL PREDICTION MODEL TO THE INFRARED WAVELENGTH RANGE

The experiments performed in Section 3 show that it is not possible to accurately distinguish between chromatic and pure black in the visible wavelength range only, i.e. the wavelength range between 380 nm and 730 nm. The goal is therefore to find a method that can determine unambiguously the amount of black ink. Once this amount is known, one can then infer the amounts of the cyan, magenta and yellow inks[1, 2].

Experiments have shown that dye inks do not absorb outside the visible domain, whereas pigmented inks do. This is interesting because, in reproduction systems such as offset printing, the cyan, magenta, and yellow inks are based on dyes whereas the black ink is based on pigments. The pigmented black ink is the only one that absorbs in the near-infrared wavelength range, i.e. from 730 nm to 1100 nm. Since the measured reflection spectra remain flat between 800 nm and 1100 nm, we consider a wavelength range between 380 nm and 850 nm, which includes the specific yellow (380-490 nm), magenta (500-610 nm), cyan (620-730 nm) and pure black (740-850 nm) absorption zones.

Figure 3 shows the difference between chromatic and pure black in the visible domain only. Figure 7 shows the same spectra, but extended to the near-infrared domain. The difference is obvious and allows us to clearly discriminate the two types of black. It is therefore possible to determine the amount of pure black ink by also considering the near-infrared wavelength region. After recovering the pure black surface coverage, the surface coverages of the cyan, magenta, and yellow inks can be recovered by considering the visible region only.

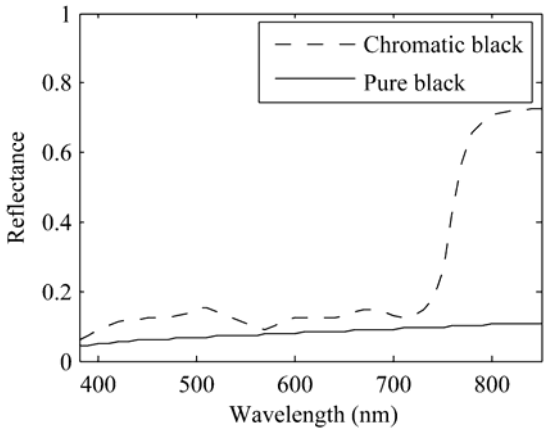

Figure 7. Reflection spectra of chromatic black and pure black prints including the near-infrared domain.

Extending the model to the near-infrared domain does not require many modifications since all the formula used in the model, e.g. Eqs. 1 and 2, are independent of the width of the wavelength range. This new EYNSN model extended to the near-infrared domain is further referred to as the *ink spreading and near-infrared enhanced Yule-Nielsen modified Spectral Neugebauer model* (IRYNSN).

We evaluate the benefits brought by the near-infrared wavelength range as follows: Given a measured spectrum, we deduce the effective ink surface coverages that reproduce this spectrum as closely as possible. These backward predictions are performed using either the EYNSN model or the IRYNSN model. Then, using the IRYNSN model, we predict the reflection spectrum from the deduced effective coverages. We finally compute two different root mean square errors (RMSE) between the measured and predicted spectra. The first RMSE is computed considering only the visible wavelength range, i.e. between 380 nm and 730 nm. The second RMSE is computed considering the visible and near-infrared wavelength range, i.e. between 380 nm and 850 nm. Using this method for the 750 colors selected in Section 1, we collect two sets of 750 RMSE for each model. The results are summarized in Table 1.

Table 1. Average, maximum and standard deviation of the root mean square errors of the 750 colors selected in Section 1 when fitting surface coverages in the visible domain only or in the visible and near-infrared domains.

RMSE in the visible domain only

	EYNSN	IRYNSN
Mean	0.0097	0.0114
Max	0.0839	0.0788
Std dev	0.0101	0.0098

RMSE in the visible and near-infrared domains

	EYNSN	IRYNSN
Mean	0.0242	0.0104
Max	0.1700	0.0689
Std dev	0.0234	0.0086

When computing the RMSE in the visible domain only, both EYNSN and IRYNSN provide low errors, i.e. the measured and predicted spectra are closely matched. When computing the RMSE in both the visible and near-infrared domains, the RMSE increases by a factor of 2.4 for the EYNSN model and remains constant for the IRYNSN model. The increase is caused by the lack of accuracy of the EYNSN model when performing backward predictions. The effective ink surface coverages that it finds match the measured spectrum in the visible domain, but are not accurate enough to match the measured spectrum in the near-infrared domain. Extending the considered wavelength range to the near-infrared domain by using the IRYNSN model provides a greater accuracy for backward predictions, which is confirmed by the low RMSE both in the visible domain alone and in the visible and near-infrared domains.

We then perform the same experiment using only the 245 colors selected in Section 3 and summarize the results in Table 2. It occurs that the considerations made for Table 1 are also valid for Table 2. The only difference is that the maximum and standard deviation values drop significantly when considering only 245 colors. We explain this behavior in the next section in the light of another experiment.

Table 2. Average, maximum and standard deviation of the root mean square errors of the 245 colors selected in Section 3 when fitting surface coverages in the visible domain only or in the visible and near-infrared domains

RMSE in the visible domain only

	EYNSN	IRYNSN
Mean	0.0083	0.0106
Max	0.0290	0.0325
Std dev	0.0038	0.0045

RMSE in the visible and near-infrared domains

	EYNSN	IRYNSN
Mean	0.0251	0.0098
Max	0.1685	0.0300
Std dev	0.0243	0.0043

In Figure 8, we show the resulting spectra when performing the above experiment with a color composed of 75% cyan, 25% magenta, 75% yellow and 30% black. On the left-hand side, the backward prediction is performed using the EYNSN model. We see that the resulting spectrum matches well the measured spectrum in the visible wavelength range, i.e. from 380 nm up to 730 nm, but diverges in the near-infrared wavelength range. Since only the black ink absorbs in the near-infrared domain, the effective black ink surface coverage is not accurate. On the other hand, if the backward prediction is performed using the IRYNSN model, the resulting spectrum matches well the measured spectrum for the full wavelength range.

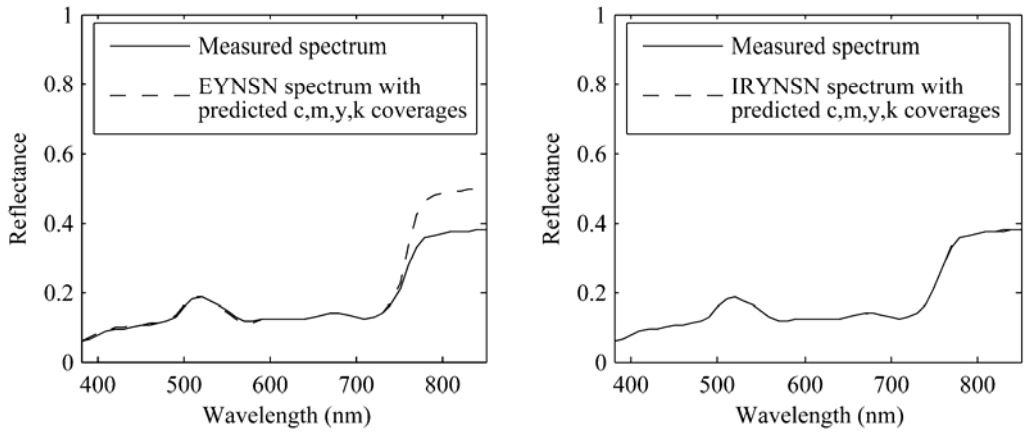

Figure 8. Comparison of the spectra resulting from backward predictions using either the EYNSN model or the IRYNSN model. The measured spectrum corresponds to a color composed of 75% cyan, 25% magenta, 75% yellow, and 30% black.

5. COMPARING FORWARD AND BACKWARD PREDICTIONS

In the preceding section, we have shown that extending the EYNSN model to the near-infrared wavelength range yields more accurate backward predictions. Such predictions allow deducing effective ink surface coverages from measured spectra. We now compare these backward predictions with forward predictions (see Figure 2). The comparison between forward and backward predictions is based on the differences between the effective ink surface coverages computed by forward predictions, or simply *effective coverages*, and the ones deduced by backward predictions, or *fitted effective coverages*.

We proceed as follows: First, the four fitted effective ink surface coverages of a given color halftone patch are deduced from the measured reflection spectrum of this color. These fitted coverages are then compared to the effective ink surface coverages given by the forward prediction model. Finally, the respective absolute difference between fitted and effective coverages of cyan (Δc), magenta (Δm), yellow (Δy), and black (Δk) are computed. With the 750 colors selected in Section 1, we have 750 sets of differences. The results are summarized in Table 3 for the EYNSN and IRYNSN models. Note that the tone reproduction curves of the EYNSN model are calibrated in the visible domain only and the ones of the IRYNSN model are calibrated in both the visible and near-infrared domains.

We can see that the effective ink surface coverages differences are lower when using the IRYNSN model than when using the EYNSN model. This means that the IRYNSN model is more consistent than the EYNSN model in regards to forward and backward predictions. Moreover, since forward predictions are known to yield good results for both the

EYNSN and the IRYNSN models[1, 2], the fitted effective coverages deduced by the IRYNSN model are more accurate than the fitted effective coverages deduced by the EYNSN model.

Table 3. Coverage differences between fitted and effective surface coverages for the EYNSN model (on the left-hand side) and the IRYNSN model (on the right-hand side) when considering the 750 colors selected in Section 1.

	Visible only (EYNSN)					Visible and near-infrared (IRYNSN)				
	Δc	**Δm**	**Δy**	**Δk**		**Δc**	**Δm**	**Δy**	**Δk**
Mean	0.0254	0.0286	0.0536	0.0274	**Mean**	0.0112	0.0184	0.0521	0.0162
Max	0.2944	0.5227	0.7243	0.1912	**Max**	0.1138	0.0961	0.7013	0.1026
Std dev	0.0394	0.0606	0.0813	0.0309	**Std dev**	0.0152	0.0212	0.0906	0.0207

It is also interesting to note that the differences in yellow effective coverages are significantly higher than the differences of the other inks. They also do not significantly decrease when fitting the surface coverages in the near-infrared domain. We suspect that this is due to the fact that yellow ink scatters light and that the superposition of yellow and other inks is not consistent across different halftones.

We then compute the coverage differences only for the 245 colors selected in Section 3 and summarize the results in Table 4. Again, we see that the IRYNSN model is more consistent than the EYNSN model since its coverage differences are lower. The yellow coverage differences are still higher than the differences of the other inks, but extending the EYNSN model to the near-infrared domain divides the yellow coverage differences by a factor of two. This tends to confirm the assumption that the superposition of yellow and other inks is not consistent across different halftones. The criterion used to select the 245 colors used in this experiment indeed limits the amount of superposed inks and therefore the inconsistencies caused by such superpositions.

Limiting the experiment to the 245 colors also affects the maximum and standard deviation values, which significantly drop. This is another confirmation of the previous assumption. Moreover, it explains why the maximum and standard deviation values in Table 2 are lower than in Table 1. Since the models handle the 245 color set better than the 750 color set, the errors they make are more focused around the mean value.

Table 4. Coverage differences between fitted and effective surface coverages for the EYNSN model (on the left-hand side) and the IRYNSN model (on the right-hand side) when considering only the 245 colors selected in Section 3.

	Visible only (EYNSN)					Visible and near-infrared (IRYNSN)				
	Δc	**Δm**	**Δy**	**Δk**		**Δc**	**Δm**	**Δy**	**Δk**
Mean	0.0222	0.0191	0.0391	0.0240	**Mean**	0.0075	0.0133	0.0197	0.0069
Max	0.1854	0.1728	0.3363	0.1912	**Max**	0.0404	0.0851	0.1522	0.0671
Std dev	0.0274	0.0258	0.0413	0.0330	**Std dev**	0.0083	0.0168	0.0243	0.0094

6. CONLUSION

We have introduced the ink spreading enhanced Yule-Nielsen modified Spectral Neugebauer model used for recovering cyan, magenta, yellow, and black ink surface coverages from reflection spectra. We have shown the difficulty in trying to deduce ink surface coverages due to the redundancy between pure and chromatic black when using the visible wavelength range only. Since the pigmented black ink absorbs in the near-infrared wavelength range whereas the cyan, magenta, and yellow inks do not, we propose to extend the measurements to the near-infrared domain. We then show that extending the EYNSN model improves the accuracy of deducing effective ink surface coverages. Finally, we show that the new IRYNSN model is more consistent than the EYNSN since forward and backward predictions yield effective ink surface coverages that are closer.

Although some inconsistencies remain, the accuracy reached by the IRYNSN model makes it a suitable building stone for applications that require backward predictions. One example of such an application is the recovery of the gray component replacement strategies from halftone patches.

ACKNOWLEDGMENT

We thank Dr. M. Riepenhoff from WIFAG AG, Bern, for having pointed to the possibility of using the near-infrared domain to distinguish between pure and chromatic black.

The Swiss National Science Foundation gave a partial support for this research under grant 200020-105119. We also thank the Swiss Innovation Promotion Agency for its support under grant KTI 6498.1 EN ET.

REFERENCES

1. R. D. Hersch, P. Emmel, F. Collaud, F. Crété, “Spectral reflection and dot surface prediction models for color halftone prints”, Journal of Electronic Imaging 14(03), 33001-12 (2005)
2. R. D. Hersch, F. Crété, “Improving the Yule-Nielsen modified spectral Neugebauer model by dot surface coverages depending on the ink superposition conditions”, *Proceedings of SPIE* vol. 5667, 434-445 (2005)
3. D.R.Wyble, R.S. Berns, “A Critical Review of Spectral Models Applied to Binary Color Printing”, Journal of Color Research and Application 25(1), 4-19 (2000)
4. R. Balasubramanian, “Optimization of the spectral Neugebauer model for printer characterization”, Journal of Electronic Imaging 8(2), 156-166 (1999)
5. T. Ogasahara, “Verification of the Predicting Model and Characteristics of Dye-Based Ink Jet Printer”, Journal of Imaging Science and Technology 48(2), 130-137 (2004)
6. J.A.C. Yule, W.J. Nielsen, “The penetration of light into paper and its effect on halftone reproductions”, *Proc. TAGA* vol. 3, 65-76 (1951)
7. J.A.S Viggiano, “Modeling the Color of Multi-Colored Halftones”, *Proc. TAGA*, 44-62 (1990)
8. H.E.J. Neugebauer, “Die theoretischen Grundlagen des Mehrfarbendrucks”, Zeitschrift fuer wissenschaftliche Photographie vol. 36, 36-73 (1937), reprinted in Neugebauer Seminar on Color Reproduction, SPIE vol. 1184, 194-202 (1989)
9. M.E. Demichel, Procédé vol. 26, 17-21 (1924)
10. A. Murray, “Monochrome reproduction in photoengraving”, J. Franklin Institute vol. 221, 721-724 (1936)
11. H.R. Kang, “Applications of color mixing models to electronic printing”, Journal of Electronic Imaging 3(3), 276-287 (1994)
12. R.D. Hersch, F. Collaud, P. Emmel, “Reproducing color images with embedded metallic patterns”, *Proc. SIGGRAPH* (2003), *ACM Trans. on Graphics* 22(3), 427-436 (2003)
13. K. Iino, R.S. Berns, “Building color management modules using linear optimization I. Desktop”, Journal of Imaging Science and Technology 42(1), 79-94 (1998)
14. K. Iino, R.S. Berns, “Building color management modules using linear optimization II. Prepress system for offset printing”, Journal of Imaging Science and Technology 42(2), 99-114 (1998)
15. A. U. Agar and J. P. Allebach, “An Iterative Cellular YNSN Method for Color Printer Calibration”, *Proc. of the 6th IS&T/SID Color Imaging Conference*, Scottsdale AZ, 197-200 (1998)
16. S. Zuffi, R. Schettini, “An innovative method for spectral-based printer characterization, Color Imaging: Device-Independent Color, Color Hardcopy, and Applications VII”, *Proc. of SPIE-IS&T Electronic Imaging* vol. 4663 (R. Eschbach, G.G. Marcu eds.), 1-7 (2002)
17. J.C. Lagarias, J.A. Reeds, M.H. Wright, P.E. Wright, "Convergence Properties of the Nelder-Mead Simplex Method in Low Dimensions," SIAM Journal of Optimization 9(1), 112-147 (1998)
18. The Mathworks Inc., http://www.mathworks.com/access/helpdesk/help/toolbox/optim/ug/fmincon.html
19. G. Sharma, “Digital Color Imaging Handbook”, Chapter 1, 35-36, CRC Press, 2003